Handbook of Star Forming Regions Vol. I
Astronomical Society of the Pacific, 2008
Bo Reipurth, ed.

The σ Orionis Cluster

Frederick M. Walter
Stony Brook University
Stony Brook, NY 11794-3800, USA

William H. Sherry
National Solar Observatory
Tucson AZ, USA

Scott J. Wolk & Nancy R. Adams
Center for Astrophysics
Cambridge MA 02139, USA

Abstract. The σ Orionis cluster is the group of stars surrounding the high mass σ Ori stellar system. It is kinematically distinct from the Orion OB1a and OB1b associations, against which it is projected. The cluster could contain up to $\sim$700 stars and substellar mass objects, with a total mass of about 225 $M_\odot$ within a radius of about 30 arcmin. The age is 2–3 million years. The distance, from main sequence fitting corrected for the sub-solar metallicity, is 420$\pm$30 pc. The mass function is similar to the field star mass function, and has been traced well into the planetary mass regime. The disk fraction is normal for its age. The cluster appears to be an older and less massive analog of the Orion Nebula Cluster.

1. Introduction

Although Herschel (1811) included the region around the third magnitude star σ Orionis in his list of nebulosities, it has only been in the past decade that this region has gained some prominence as a distinct star formation region. The star σ Ori is situated well inside the boundaries of the Orion OB1 association (Blaauw 1991), some 2 deg southwest of ζ Ori, the easternmost of the three supergiants that make up the belt of Orion. The east side of Orion OB1 abuts the Orion B molecular cloud. σ Ori and its surroundings are projected against a diffuse Hα nebulosity (probably Herschel's cloud), which reaches peak brightness in the vicinity of ζ Ori and along the dark cloud hiding NGC 2023/2024 (see Figure 1).

The Orion OB1 association has been recognized for a long time as a region of high mass star formation. In the past 2 decades has come the realization that OB associations are also regions of copious low mass star formation (e.g., Walter et al. 2000, Briceño et al. 2007). Garrison (1967) discussed the "σ Orionis clustering", and Lyngå (1981) catalogued a cluster (C0536-026) here. X-ray observations later showed an apparent clustering of sources centered near σ Ori (Walter et al. 1997; Walter, Wolk, & Sherry 1998). Followup observations have confirmed that there exists a small cluster of low

Figure 1. The region surrounding σ Ori. North is up, east is to the left. The other bright stars are ζ Ori to the upper left and ϵ Ori (upper right). The red is diffuse Hα emission. The Horsehead is visible east of σ Ori, while the Flame Nebula (NGC 2024) is east of ζ Ori. Courtesy Robert Gendler.

mass stars associated with σ Ori, embedded within or projected against the larger OB association. This we have called the σ Ori cluster.

Our aim here is to present an overview, focussing on the important characteristics of the cluster, With a few exceptions, we do not comment on the properties of individual stars. We do not supply a list of members, aside from the brightest stars.

2. Overview of Fossil Star Formation in Orion OB1

Orion OB1 (Blaauw 1964, 1991) is a well studied nearby example of an OB association. OB associations (Ambartsumian 1947) are young, gravitationally unbound groups of stars defined by a population of high mass stars. Associations are often large on the sky; the stellar densities are not sufficient to gravitationally bind these associations against galactic tides (Bok 1934). OB associations are only recognizable for a few tens of millions of years, until the highest mass stars burn out and the fainter stars are absorbed into the field.

Ambartsumian recognized that the O and B stars were short-lived, and could not have moved far from their birthplaces in a few million years, so such a grouping of high mass stars must mark a region of recent star formation. Active star formation, manifested by embedded infrared sources, active accretion, and prominent circumstellar disks, generally occurs only over a period of a few million years; older associations are generally no longer forming stars. These older OB associations are fossil star forming regions. They retain most of the end-products of the star formation process. The accretion process is complete (except perhaps for the lowest mass objects): all stars have attained their ultimate masses. The gas and dust of the stellar nursery has dissipated, blown away by the hot star winds or supernova shocks, revealing all members, even at short wavelengths.

The Orion OB1 association covers an enormous extent on the sky, most prominently in the belt of Orion and the Orion Nebula. The association has been divided into four sub-associations (Blaauw 1964). Within the association we see a wide range of conditions, from fossil regions (Ori OB1a) to regions of active on-going star formation (Orion OB1d - the Orion Nebula Cluster). The association has been discussed, and its components defined, by Blaauw (1964, 1991), Warren & Hesser (1977a, 1977b, 1978), Brown et al. (1994), and de Zeeuw et al. (1999).

3. The Massive Stars

The trapezium system σ Ori (Figure 2) is considered a member of the Orion OB1b subassociation. The A and B components form a 0.25 arcsec visual binary (ADS 4241; BU 1032 AB). The orbit (Heintz 1997) has been refined using speckle observations (Hartkopf et al. 1996); the period is 155 years. Frost & Adams (1904) suspected σ Ori (presumably AB) of having a variable radial velocity . The A component is a double-lined spectroscopic binary (Bolton 1974) with about a 140 day period and a highly eccentric orbit (Peterson et al. 2008). The Aa component is about 0.5 mag brighter than Ab. The C, D, and E components share a common proper motion with σ Ori AB, and are likely physical companions. σ Ori E (V1030 Ori) is a magnetic B star (Greenstein & Wallerstein 1958; Landstreet & Borra 1978).

It is σ Ori, not ζ Ori, that illuminates the Horsehead nebula (Reipurth & Bouchet 1984). Abergel et al. (2003) concluded, based on ISOCAM observations, that the rim of the Horsehead is a photodissociation region illuminated edge-on, and that σ Ori and the Horsehead must be about the same distance from Earth. Based on its extinction, and the Hipparcos parallaxes, ζ Ori appears to be in the foreground.

In all, there are 19 stars with $V < 11$ mag within 30 arcmin of σ Ori AB (Table 1). Based on positions in the color-magnitude diagram, 15 of these appear to be members of the cluster, and two others are possible members (Sherry et al. 2008). Figure 3 shows

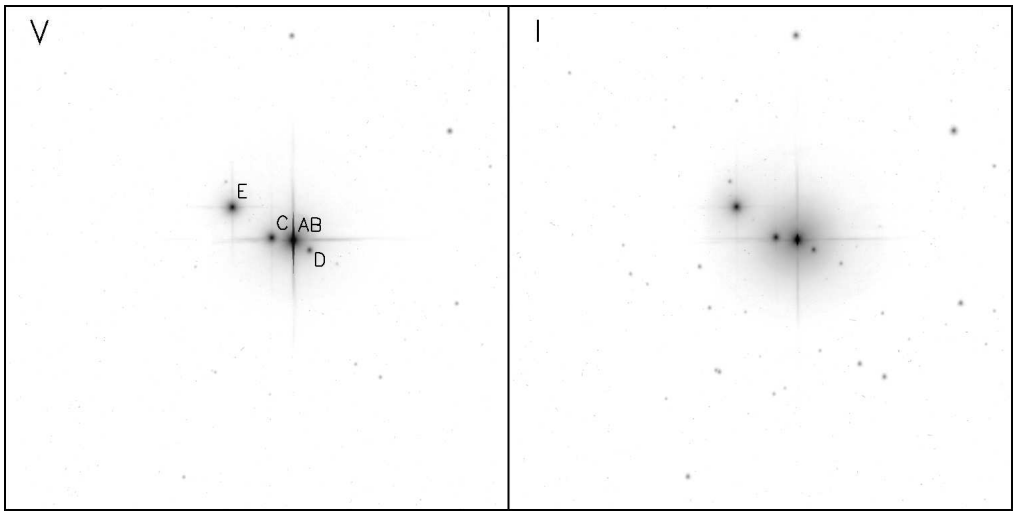

Figure 2. The center of the σ Ori cluster in the V (left) and I (right) bands. North is up, east is to the left. The components are labelled in the V band image. σ Ori AB is saturated and bleeds in the N-S direction. The images are reconstructed from about three thousand 0.2 sec integrations taken with the SMARTS/CTIO 0.9m reflector, shifted and added to improve spatial resolution. Each field covers about 5 arcmin on a side. The scaling is logarithmic. Caballero (2005) shows a similar figure in the $J + H$ band.

that the members define a narrow zero-age main sequence (ZAMS). Stars with spectral types later than about A0 lie above the ZAMS. Caballero (2007a) examined the 41 stars in common between the Tycho-2 and 2MASS catalogs that lie within 30 arcmin of σ Ori AB. He found 26 likely members and 4 candidate members in 23 stellar systems with masses $>$1.2 $M_\odot$. For the cooler stars in the sample, Caballero based membership criteria on indicators of youth, including strong X-ray emission, near-IR excesses, Hα emission, and Li absorption.

4. The Distance to the σ Orionis Cluster

The Hipparcos parallax of σ Ori is 2.84$\pm$0.91 mas (Perryman et al. 1997). Consequently, many authors adopt the 352 pc best distance to σ Ori as the distance to the cluster. This is not a well-determined distance: this parallax places σ Ori between 260 pc and 520 pc from the Sun at 68% confidence. Caballero (2008b) derived a dynamical distance for σ Ori AB of 334^{+25}_{-22} pc, assuming the stars are single (see Sect. 3.) and the age is 3 Myr.

If σ Ori is a member of the Ori OB1b association, one can use the better-constrained distance to the association as an estimate of the distance to σ Ori and its cluster. De Zeeuw et al. (1999) used the Hipparcos parallaxes to determine a mean distance of 473$\pm$33 pc for the OB1b association. The authors noted that the actual uncertainty is larger than the formal uncertainty of 33 pc because they had to use a simplified membership selection due to the small proper motions of association members. This

Table 1. All the stars with V magnitudes<11.0 that lie within distance r <30 arcmin of σ Ori AB. The sources of the magnitudes, colors, and spectral types are compiled by Sherry et al. (2008). These stars are plotted on Figure 3. HD 294273 and HD 294279 are non-members because they cannot be dereddened back to the best fit main sequence. The observed $B-V$ color of the triple system σ Ori Aab+B is –0.24. The spectral type of σ Ori Ab is estimated from its V magnitude. HD 37333 and HD 294272 are overluminous, with dereddened colors and magnitudes consistent with a distance of ∼350 pc. This makes them possible members of the Orion OB1a association at ∼330 pc (de Zeeuw et al. 1999), or binary systems with approximately equal luminosity components. Caballero (2005) found HD 37525 to be a close binary with a 0.5 mag difference at H. HD 37564, which has a 24μm excess (Hernández et al. 2007), is too bright to be a member even in an equal mass binary. It may be a foreground star with a debris disk.

ID	$B-V$ [mag]	V [mag]	Spectral Type	r [arcmin]	Notes
σ Ori Aa	—	4.4	O9V	0.00	
σ Ori Ab	—	4.9	[B0V]	0.00	
σ Ori B	—	5.16	B0.5V	0.00	
σ Ori C	—	9.42	A2V	0.20	
σ Ori D	–0.18	6.81	B2V	0.22	
σ Ori E	–0.18	6.66	B2Vp	0.69	variable
HD 294272	0.03	8.48	B9.5III	3.12	OB1a or binary
BD –02 1323C	–0.04	8.77	B8V	3.25	
HD 294271	–0.11	7.91	B5V	3.47	
HD 37525 AB	–0.09	8.08	B5V	5.11	
HD 294273	0.26	10.66	A7-9	8.68	non-member
HD 37564	0.23	8.46	A5-7	8.74	non-member
HD 37633	0.03	9.04	B9	16.00	V1147 Ori
HD 37333	0.06	8.52	A0V	18.60	OB1a or binary
HD 294279	0.39	10.72	F3	19.34	non-member
HD 294275	0.09	9.43	A1V	20.45	
HD 37545	–0.02	9.31	B9	21.46	
HD 37686	0.02	9.23	B9.5V	22.64	
HD 37699	–0.13	7.62	B5V	25.79	

is consistent with the 380 to 460 pc photometric distance found by Anthony-Twarog (1982) for the Warren & Hesser (1977a) b1 group.

Garrison (1967) found a distance of 440 pc by main sequence fitting of the early type stars in the area around σ Ori. Sherry et al. (2008) revisited this zero-age main sequence (ZAMS) fitting, incorporating more stars and a more detailed reddening analysis. The color-magnitude diagram of all stars with V <11 mag that lie within 30 arcmin of σ Ori AB is shown in Figure 3. The ZAMS is well defined. Fitting an empirical solar-metallicity ZAMS (from Turner 1976, 1979) yields a distance of 440±30 pc (Figure 4). The metallicity of the Orion OB1 association is sub-solar, with [Fe/H]=-0.16 ± 0.11 (Cunha, Smith, & Lambert 1998). The effect of lower metallicity is to shift the ZAMS (e.g., Cameron 1985; Pinsonneault 2004), and decrease the geometric distance to about 420 pc. This is significantly larger than the 350–360 pc used in many analyses, and is

consistent with the mean parallactic distance to Ori OB1b. The σ Ori cluster may be foreground to the bulk of the Orion OB1b association.

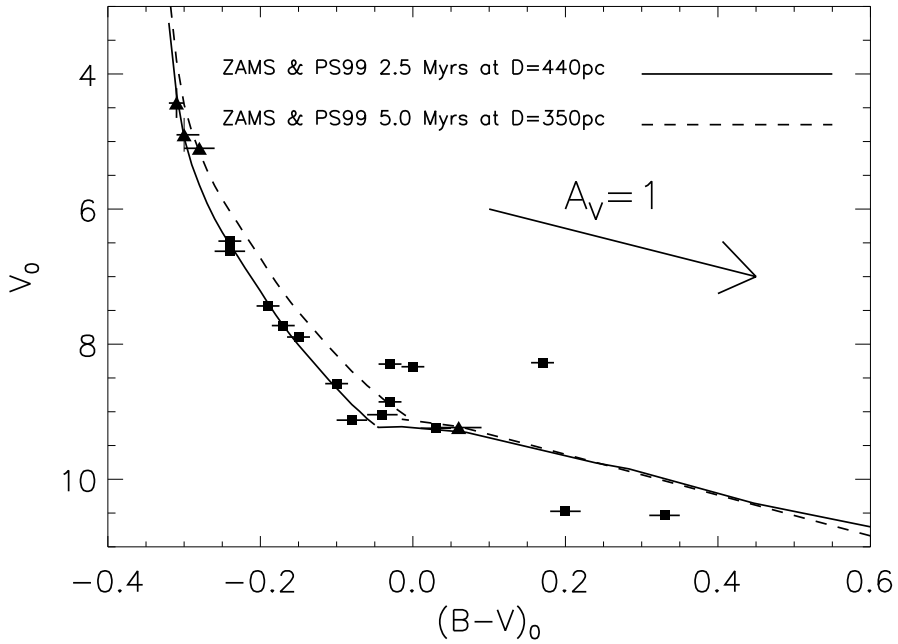

Figure 3. The de-reddened color-magnitude diagram of stars with V <11 mag within 30 arcmin of σ Ori AB (see Table 1). The two stars fainter than V=10 mag are non-members. Triangles mark the positions of σ Ori Aa, Ab, B, and C, for which the intrinsic $B-V$ colors are estimated from spectral types. The solid and dashed lines are the empirical solar-metallicity zero-age main sequence (Turner 1976) plus a 2.5 Myr or 5.0 Myr isochrone from Palla & Stahler (1999), shifted to respective distances of 440 and 350 pc.

5. Low Mass Cluster Membership

The cluster is not obvious on the sky, because it is not silhouetted on a dark cloud, and the background contamination is significant. We initially recognized this as a possible cluster from the density of X-ray sources surrounding σ Ori. Many groups have followed up with photometric and spectroscopic studies in the optical and near-IR. Note that most of the source membership statistics listed below refer solely to the investigations in question; there is as yet no completed meta-analysis providing the definitive cluster statistics.

5.1. X-ray Selection

A small number of X-ray sources were detected near σ Ori by the *EINSTEIN* Observatory. Followup optical spectroscopy (Wolk 1996) showed that many of these were low

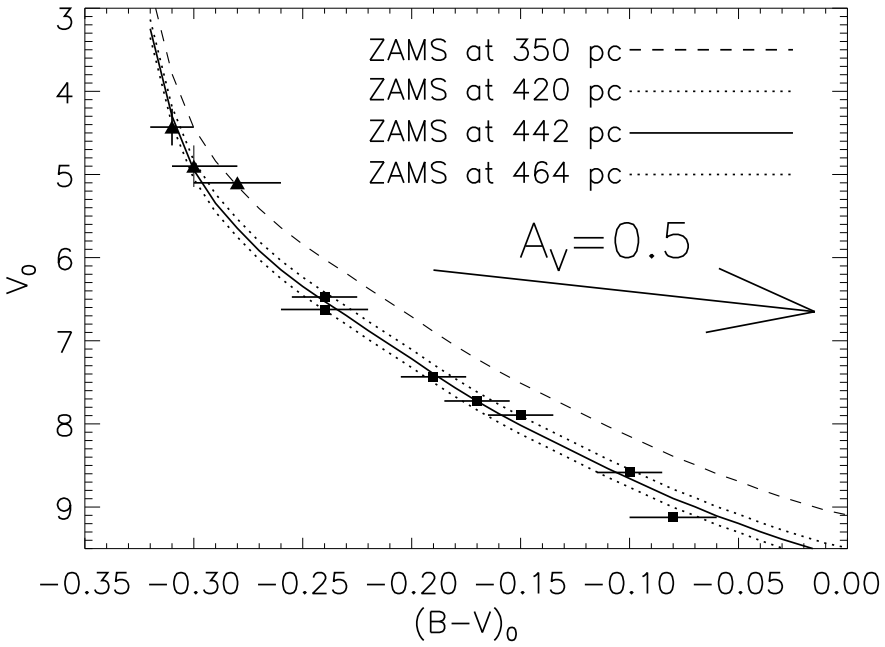

Figure 4. The de-reddened color-magnitude diagram of the O and B type cluster members (Table 1). Triangles mark the positions of σ Ori Aa, Ab, B, and C, for which the intrinsic $B-V$ colors are estimated from spectral types. The lines are the empirical solar-metallicity zero-age main sequence of Turner (1976) shifted to the indicated distances. The A_V=0.5 mag reddening vector for R=3.1 is shown; the mean reddening is E($B-V$)=0.06 mag. The dotted lines show the formal $\pm$22 pc uncertainty on the best fit distance. Our quoted $\pm$30 pc uncertainty include uncertainties in the ZAMS calibration. The best fit distance is 442$\pm$30 pc, assuming solar metallicities. σ Ori B lies about 0.5 mag above the ZAMS and may be an unrecognized binary system.

mass pre-main sequence (PMS) stars, based on the presence of Li I λ6707Å absorption. Most did not have Hα in emission above the continuum, and so are classified as naked (or weak-lined) T Tauri stars.

ROSAT pointed observations showed the presence of an apparent clustering of about 100 X-ray sources within 1 degree of σ Ori (Walter, Wolk, & Sherry 1998). Berghöfer & Schmitt (1994) and Sanz-Forcada et al. (2004) discussed the X-ray emission from σ Ori itself. Groote & Schmitt (2004) discussed the X-ray emission from σ Ori E. Mokler & Stelzer (2002) identified three brown dwarf candidates (spectral type M5$-$6) in the σ Ori cluster with ROSAT X-ray sources.

Franciosini et al. (2006) presented a 43 ksec XMM-Newton image of this cluster, identifying 88 of the 175 X-ray sources, including at least one brown dwarf candidate, with cluster members. Their limiting sensitivity is log(L_X)$\sim$28.3 at the center of the field, and log(L_X)$\sim$28.6 13 arcmin off-axis, assuming a 350 pc distance; at our preferred 420 pc distance, their limiting luminosities are 0.2 dex larger. The median value

of log($\frac{L_X}{L_{bol}}$) of –3.3 is near the saturation limit for cool star coronae, and is higher than seen in other young clusters, such as the ONC. They attributed this to an increase in log($\frac{L_X}{L_{bol}}$) with age to about 4 Myr, where it saturates (Flaccomio et al. 2003). They observed half the PMS stars to be significantly variable in X-rays during this observation.

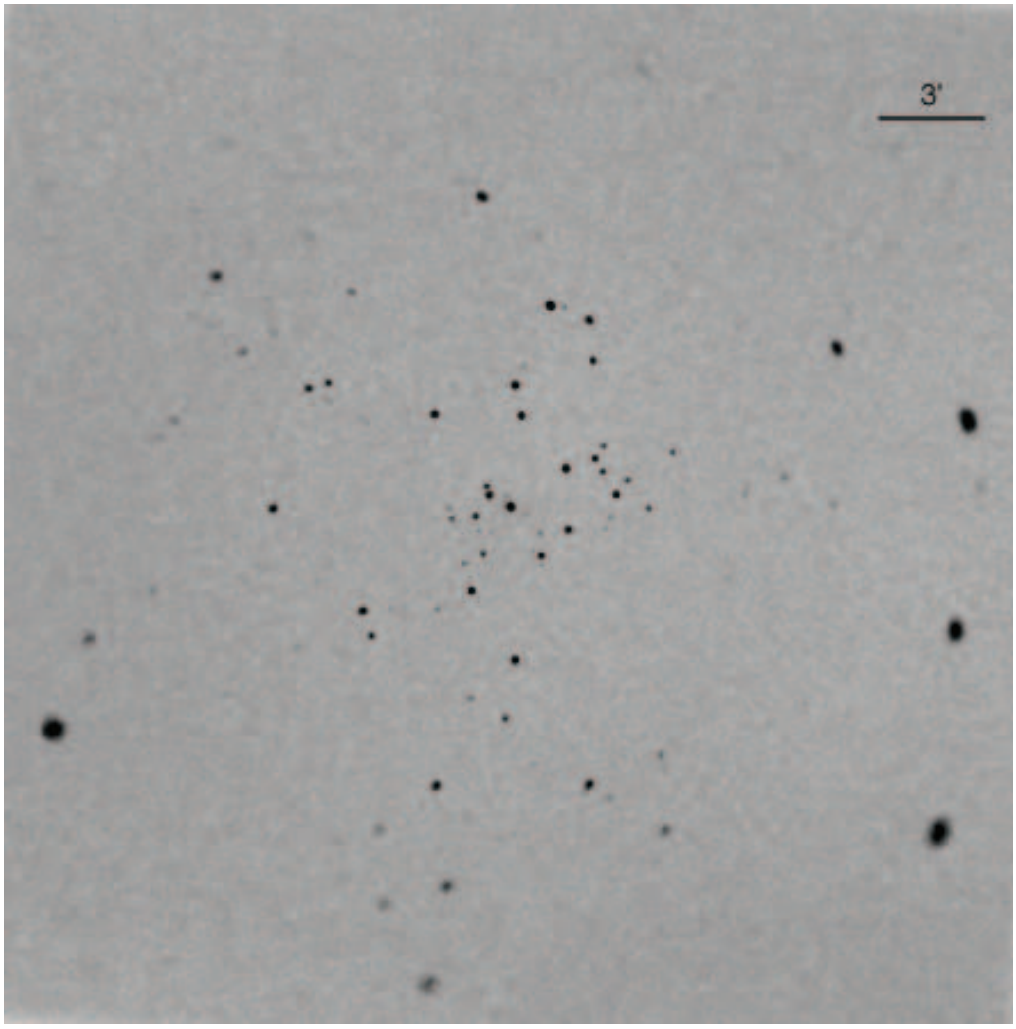

Figure 5. The full *Chandra* HRC image of the σ Ori cluster. The source at the center is σ Ori AB. The large source size off-axis reflects the off-axis degradation of the point-spread function rather than source brightness. North is up; east is to the left. The field spans about 30 arcmin.

In a 75 ksec observation by the *Chandra*/HRC, Adams-Wolk et al. (2005) detected 140 point sources in a 30 x 30 arcmin field (Figure 5). 103 of these have been confirmed as PMS stars from optical spectra or photometry consistent with cluster membership. The X-ray source list is complete to about log(L_X)=27.75, with the faintest source having log(L_X)$\sim$27.25 (at 420 pc). Three X-ray sources are confirmed non-members of the cluster. Of the confirmed cluster members with spectra, 18% (7/40) have strong Hα

emission signatures or other indications of an active disk. Very few stars in this region have JHK excesses characteristic of disks (Figure 6; but see Sect. 6.8.). The full *Chandra*/HRC field contains over 2800 2MASS sources. In the central 4 arcmin (the sensitivity of HRC falls off quickly outside this region) only 10 of the 62 2MASS sources are associated with *Chandra* X-ray sources, the faintest of these having K=13.2. The brown dwarf limit for 3 Myr old stars at a distance modulus of 8.2 is about K=14 mag based on the Baraffe et al. (1998) tracks, so none of these sources can be substellar.

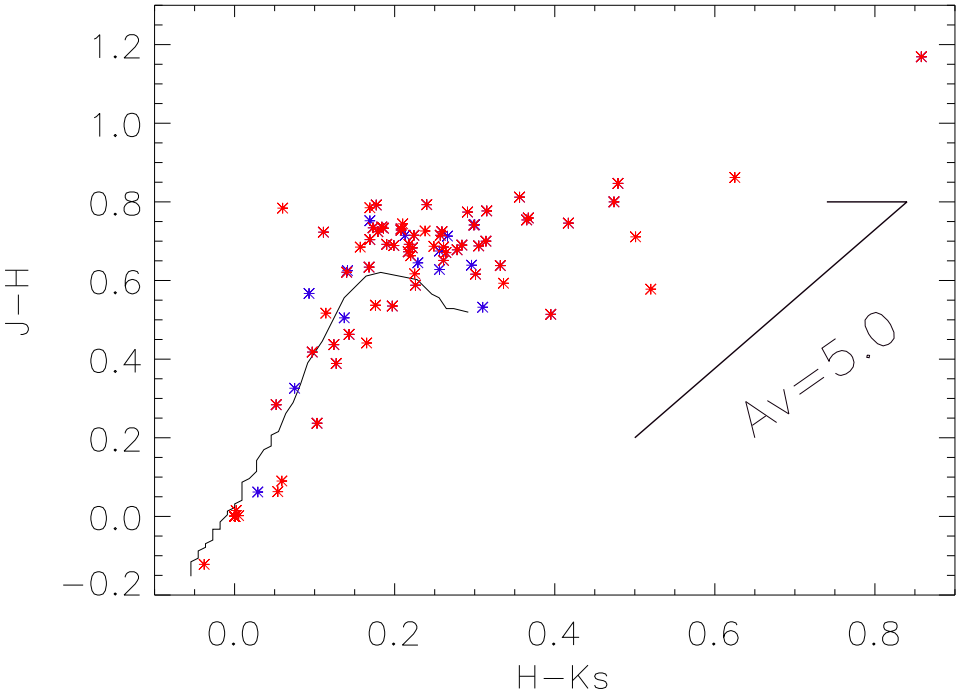

Figure 6. The near-IR color-color diagram for the *Chandra* HRC X-ray sources. The IR colors are taken from the 2MASS catalog. X-ray source counterparts are shown in red (σ Ori cluster members) and blue (non-members); The thin line represents the locus of unreddened main sequence photospheric colors. Only a few stars, those which lie to right of the extrapolation of the reddening vector from the end of the unreddened main sequence, show significant $H - K_s$ color excesses. Most stars exhibit main sequence colors with about 0.2 magnitudes of reddening.

5.2. Optical/IR Selection

Objective prism surveys within Orion (Haro & Moreno 1953; Nakano et al. 1995; Wiramihardja et al. 1989, 1991) revealed a large number of Hα emission objects. Weaver & Babcock (2004) analyzed a Curtis-Schmidt plate, and reported 63 Hα-emitting objects within about a 1 deg region around σ Ori, to a limiting magnitude of 18. By comparing their results with those from the Kiso survey, and accounting for the expected stellar variability, Weaver & Babcock extrapolated to a total population of

about 250 Hα-emitting objects, with unreddened $V \leq$16.5, corresponding to spectral types of dM0 and earlier in this region, or a mean space density of 0.86 pc^{-3}.

Many low mass PMS stars, especially those earlier than K0–K5, tend not to emit Hα above the continuum. We obtained optical spectra of many of the counterparts of the *EINSTEIN* and *ROSAT* X-ray sources (Wolk 1994; Walter et al. 1998). Of these, there are 82 likely low mass PMS stars within 30 arcmin of σ Ori. Twenty eight other, non-X-ray-selected stars, were also found to be low mass PMS stars.

Walter et al. (1998) obtained spectra of 258 stars selected from the HST Guide Star catalog within 30 arcmin of σ Ori and with $V <$15 mag. Of these, 22% are PMS stars (spectral types G and K). If the Guide Star Catalog is complete to V=15 mag in this region, this suggests a space density of 120 PMS stars per deg^2 in the range 10$< V <$15 within 30 arcmin of σ Ori, and a total population of about 90 low mass stars in this magnitude range.

Sherry et al. (2004) surveyed a 0.89 deg^2 region around σ Ori photometrically in VR_CI_C. They used V magnitudes and $V-I_C$ colors to estimate membership probabilities for stars with 15$\leq$V$\leq$19 (Figure 7). Membership probabilities were calculated by fitting the number of stars in bins along a number of cross-sections through the color-magnitude diagram with the sum of a Maxwellian-like distribution of field stars and a Gaussian distribution of cluster members as a function of $V - I_C$ color. This allowed the authors to estimate both the number of cluster members and the number of field stars at each point along the cluster locus.

Kenyon et al. (2005) obtained spectra of 76 photometrically-selected low mass candidates (54 of which are not included in the Sherry et al. sample). They found that over 2/3, and perhaps as many as 90%, are clearly PMS members of the cluster.

Figure 8 shows the spatial distribution of the known low mass (spectral types G and later) members of the cluster. It includes all the stars for which Sherry et al. (2004) estimated membership probabilities in excess of 80%, as well as the stars from Kenyon et al. (2005) that are not clear non-members. It also includes spectroscopic PMS stars (Walter et al. 1998) within 40 arcmin of σ Ori. It does not include the fainter objects from Béjar et al. (2004a; 2004b) or Caballero et al. (2007).

Hernández et al. (2007) surveyed the area with the *Spitzer* Space Telescope. Using the IRAC colors (primarily to exclude galaxies) and 2MASS and V-band magnitudes, they identified 1280 point sources. The sample is "essentially complete" to J=14.0 mag, which corresponds to 0.15 M$_\odot$ at a distance of 440 pc and a 3 Myr age. Of these stars, they considered 336 to be members based on location in the V vs. $V-J$ and J vs. $J-K$ color-magnitude diagrams and ancillary information (X-rays, variability, optical spectroscopy). Membership of another 133 color-selected stars (mostly with 13$< J <$14 mag) is considered uncertain because of heavy contamination and a lack of ancillary information.

5.3. Contamination by Field Stars

Photometric selection of cluster members is efficient for the σ Ori cluster because the cluster locus is distinct from the bulk of the field stars along our line of sight. Yet there are field stars that lie on the cluster locus on the color-magnitude diagram. This makes it impossible to unambiguously classify any individual star as a cluster member based upon single-epoch photometry alone. Sherry (2003) indicated that the contamination is $\sim$20% (from his Figure 6.6). Sherry et al. (2004) concluded that the field star contamination in their photometrically selected sample of likely cluster members (13$< V <$20)

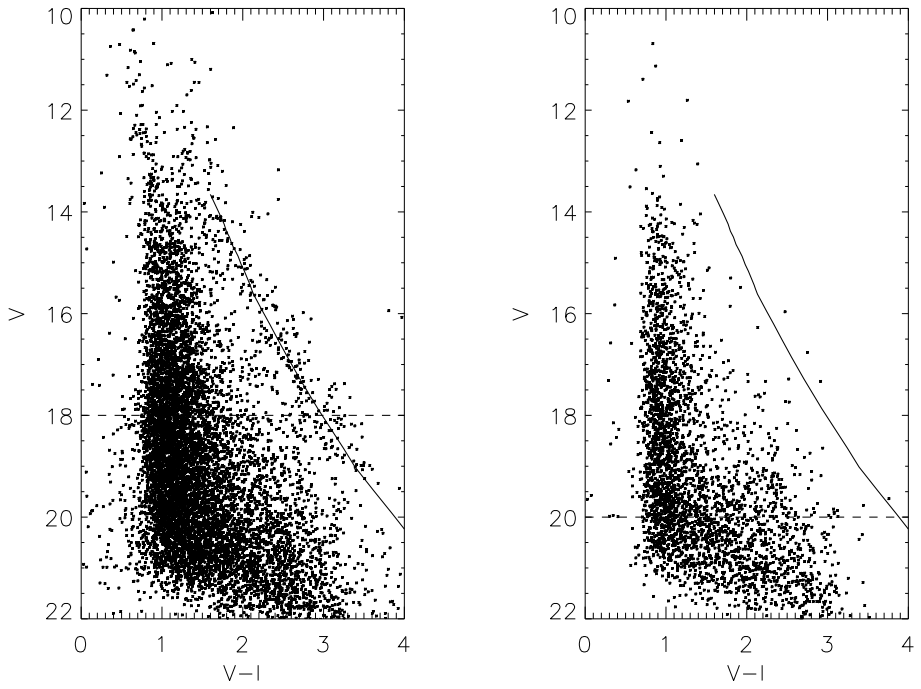

Figure 7. The left panel shows the V vs. $V-I_C$ color-magnitude diagram of 9556 stars in 0.89 deg^2 around σ Ori. The solid line is a 2.5 Myr isochrone (Baraffe et al. 1998; Baraffe et al. 2001) at a distance of 440 pc (de Zeeuw et al. 1999). This isochrone marks the expected position of the PMS locus for Orion OB1b. There is a clear increase in the density of stars around the expected position of the PMS locus. The completeness limit of these data is marked by the dashed line. The right panel shows the same color-magnitude diagram for the 0.27 deg^2 control field. The isochrone (solid line) is the same as in the left panel. The dashed line marks the fainter completeness limit of the control fields. This figure was taken from Sherry et al. (2004).

is relatively small. At lower masses (0.006$< \frac{M}{M_\odot} <$0.11), Caballero et al. (2007) estimated a 12% contamination in stars selected in the I vs. $I-J$ color-magnitude diagram.

Kenyon et al. (2005) used intermediate-resolution spectra to measure the Li I λ6708 Å and Na I λ8183/8195 Å absorption lines to confirm the youth of candidate cluster members. They found that at least 57 of the 76 stars in their sample show multiple signatures of youth and only 6 of the stars were clearly foreground M dwarfs. The remaining 13 members had at least one signature of youth (the radial velocity of the cluster, a low gravity, or enhanced Li absorption). This indicates that the level of field star contamination among photometrically selected candidate cluster members in the mass range 0.04$< \frac{M}{M_\odot} <$0.3 is 15$\pm$10%.

Burningham et al. (2005) obtained follow-up spectra of 117 additional photometric candidate cluster members from the $R_C I_C$ survey of Kenyon et al. (2005). Based upon the radial velocity distribution of their spectroscopic sample, they concluded that

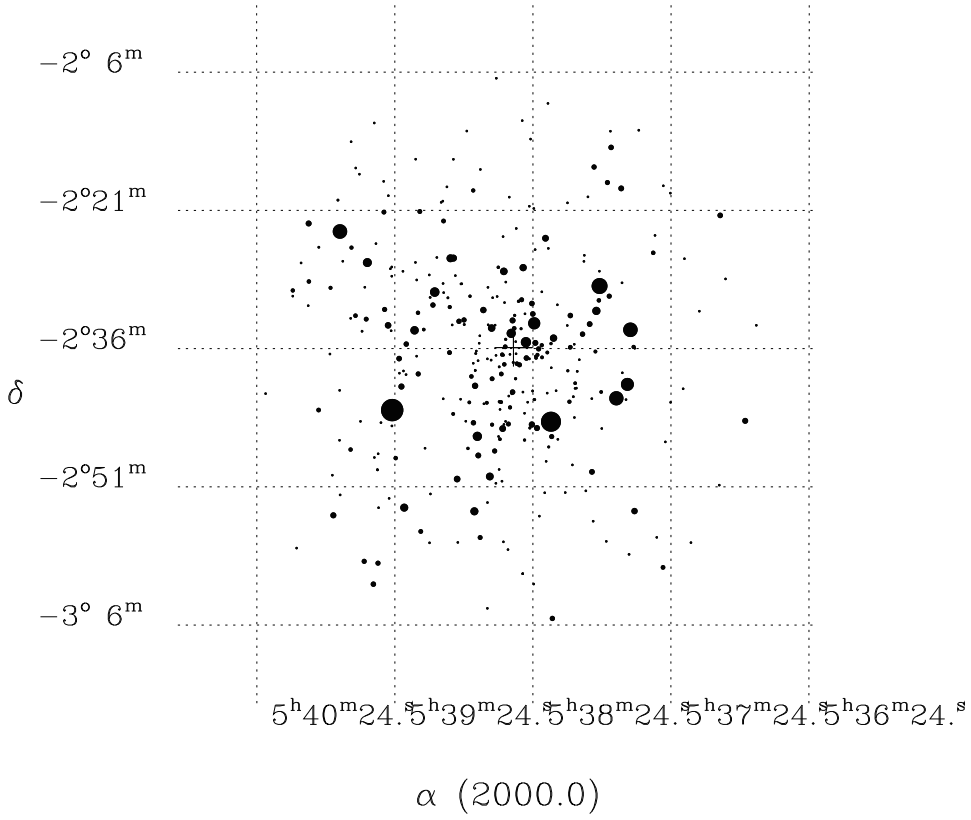

Figure 8. The low mass (spectral types GKM) members of the σ Ori cluster currently identified from spectroscopy or photometry. The size of the dot is inversely proportional to the V magnitude of the star. The brightest star plotted has V=10.4 mag. See the text for details of the completeness. The plus near the center marks the location of σ Ori.

photometric selection does not miss a significant number of cluster members and that for I <17 the cluster locus on at least the I_C vs. $R - I_C$ color-magnitude diagram has a low level of field star contamination.

A more likely, and more insidious, source of contamination is from the PMS populations of the other Orion OB1 subassociations. Brown et al. (1994) discussed the populations of the four subassociations. Because the radial velocities are similar (see Sect. 6.3.) and the proper motions are small, the populations cannot be easily distinguished kinematically. Orion OB1a is closer and older (330 pc; 10 Myr) than Orion OB1b (450 pc; 2 Myr), and so should be distinguishable statistically on the basis of a color-magnitude diagram or age indicators. The assignation of memberships of the B stars in Warren & Hesser (1977a; see also Figure 6 of Sherry et al. 2004) is solely by location on the sky, which is likely unphysical. We expect significant overlap of the foreground OB1a association in the rectangle that defines the OB1b association. Sherry et al. (2004, 2008) discussed the contamination by high mass stars (see also Table 1);

contamination by low mass members of the OB1a association was claimed by Jeffries et al. (2006; see Sect. 6.3.).

6. Cluster Properties

6.1. Spatial Structure

Sherry et al. (2004) used their sample of photometric candidate cluster members in the mass range $0.2 \leq \frac{M}{M_\odot} \leq 1.0$ with membership probabilities greater than 40% to estimate the radius and radial profile of the cluster.

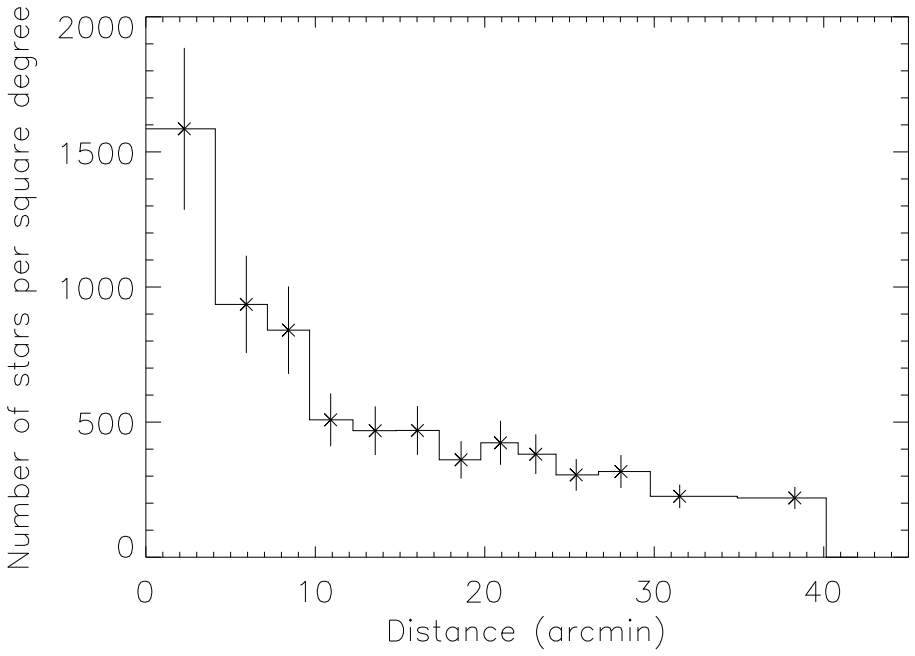

Figure 9. The radial profile of likely PMS stars, selected by optical colors, near σ Ori (Prob$_{PMS}$ $\geq$40%). This includes stars to a completeness level near V=20 (Sherry et al. 2005). The error bars are the square root of the number of stars per bin. The non-zero number density between 30 and 40 arcmin from σ Ori is the level of contamination.

The bulk of the cluster members lie within $\sim$30 arcmin of σ Ori AB. The radial profile (Figure 9) of the cluster peaks at the position of σ Ori and is consistent with a King model. The parameters of the model are not very tightly constrained by the data. Models with King radii between 0.4 and 2.0 pc and central densities ranging from 2.5 to 20 stars pc^{-3} ($0.2 \leq \frac{M}{M_\odot} \leq 1.0$) could be fit with reasonable values of χ^2_ν. Assuming the field star mass function (Kroupa 2002) the central density is about 8 stars pc^{-3}. Sherry et al. found that the density of cluster members fell below the expected level

of field star contamination at a distance of 30 to 40 arcmin from σ Ori AB. The tidal radius of the cluster was poorly constrained.

Béjar et al. (2004a) fit the radial profile of the substellar population with an exponential function $\rho = \rho_0 e^{-r/r_0}$. Their best fit exponential has ρ_0=0.26$\pm$0.03 objects arcmin^{-2} and r_0=0.09$\pm$0.06 pc (using a distance of 350 pc). This radial profile is similar to that of the low-mass stars.

Hernández et al. (2007) found the radial profile of the cluster has a FWHM of 0.25 degrees. The possible enhancement in disk fraction toward the northeast (Sect. 6.9.), in the direction of NGC 2024 and ζ Ori, may indicate contamination by a younger population.

Caballero (2008a) reported that the cluster (340 members and candidates from Caballero 2008c) consists of a core region of about 20 arcmin radius surrounded by a rarefied halo. The core can be fit with a King profile; the surface density falls off as radius^{-1}. The stars more massive than 3.7 M$_\odot$ concentrate towards the core, where there may be a deficit of low mass objects. The cluster is not azimuthally-symmetric: Caballero found an overdensity extending east from the cluster toward the region of the Horsehead Nebula. He also reported that the distribution of stars outside the core is filamentary rather than smoothly distributed. He did not discuss possible contamination from stars associated with NGC 2024.

6.2. Reddening

The low reddening of the cluster is one of the properties that makes it such a valuable site to study young stars and substellar mass objects. σ Ori has E($B-V$) of 0.05 mag (Lee 1968; Brown et al. 1994). Shull & van Steenberg (1985) quoted E($B-V$) = 0.06 mag for σ Ori E. Thirteen members of Orion OB1b within 40 arcmin of σ Ori have a median extinction E($B-V$) = 0.05 mag (Brown et al. 1994). Sherry et al. (2008) found a mean E($B-V$) of 0.06$\pm$0.005 mag, and obtained a tight de-reddened color-magnitude diagram (Figure 4) from simply assuming $(B-V)_0$ from the spectral types of the high mass members. All of these analyses have assumed A$_V$/E($B-V$) = 3.1.

The measured neutral hydrogen column density N$_{\rm H}$ along the line of sight to σ Ori is about 3.3$\times$10^{20} cm^{-2} with a 20% uncertainty (Fruscione et al. 1994; Bohlin et al. 1983). For σ Ori E the measured N$_{\rm H}$ is 4.5$\times$10^{20} cm^{-2} with an uncertainty of 20% (Fruscione et al. 1994; Shull & van Steenberg 1985). These values of N$_{\rm H}$ are consistent with E($B-V$)$\sim$0.05–0.08 using the standard ratio of total-to-selective absorption.

6.3. Radial Velocity

The radial velocity of σ Ori AB was measured at 29.2$\pm$2 km s^{-1} by Wilson (1953) and at 27 km s^{-1} by Morrell & Levato (1991). This is somewhat larger than the 23.1$\pm$1.4 km s^{-1} mean velocity of the Orion OB1b association (Morrell & Levato 1991). The measured radial velocities of probable low-mass members of the σ Ori cluster are consistent with that of σ Ori. Walter et al. (1998) found a mean radial velocity for spectroscopic members between 25 and 30 km s^{-1}. Burningham et al. (2005) measured a peak in the velocity distribution at 29.5 km s^{-1} with a range of 24–37 km s^{-1}. Kenyon et al. (2005) found a mean of 31.2 km s^{-1} for 66 low mass members and possible members. Muzerolle et al. (2003) found a mean velocity of 30.9 km s^{-1} for 6 substellar-mass objects. Zapatero Osorio et al. (2002a) found a much larger radial velocity of 37.3 km s^{-1}, also primarily for substellar mass objects.

In a more precise study, Jeffries et al. (2006) found two peaks in the radial velocity distribution of 148 low mass stars (M$<$0.5 M$_\odot$) within about 20 arcmin of σ Ori. These two kinematically-distinct populations are separated by about 7 km s^{-1} (Figure 10). They associated the higher velocity (31$\pm$0.1 km/s) group with the σ Ori cluster, and the lower velocity (23.8$\pm$0.2 km/s) group with the Ori OB1a association, based on the mean velocities and relative ages. The higher velocity group is concentrated towards σ Ori, while the lower velocity group appears spatially extended to the north. Jeffries et al. concluded that, within 10 arcmin of σ Ori, the contamination by the Ori OB1a stars is at about the 10% level. The bimodal velocity distribution has been confirmed by Maxted et al. (2008).

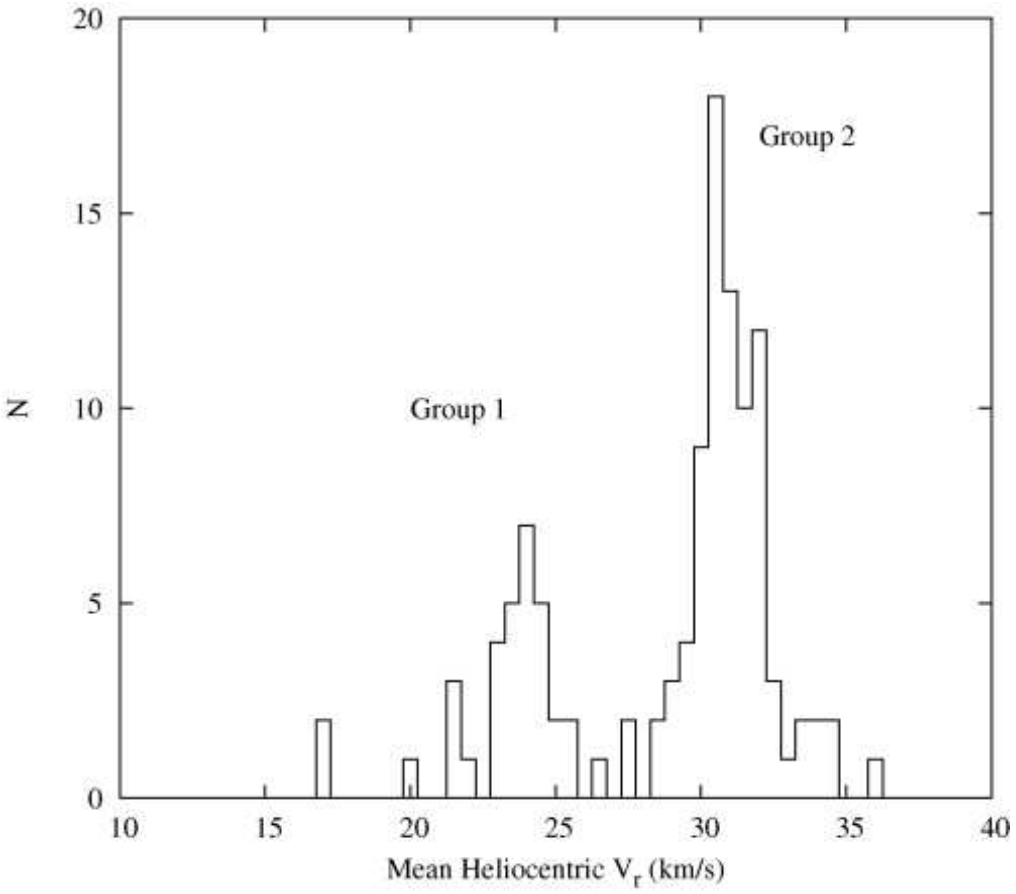

Figure 10. The distribution of radial velocities in the σ Ori cluster. Two peaks are evident. Group 2 is the σ Ori cluster; group 1 may be identified with the Ori OB1a association. (From Jeffries et al. 2006)

Sacco et al. (2007) obtained high resolution spectra of 98 candidate cluster members. They found 61 stars with radial velocities within $\pm 3\sigma$ of the cluster mean. The others stars include 12 possible binaries, one lower velocity PMS star, an apparent member of Orion OB1a or b, and 24 apparent field stars. Two of the radial velocity members appeared to be field stars (as expected statistically).

6.4. Mass Function

The σ Ori cluster is an ideal region wherein to measure the initial mass function of substellar objects because it is young, compact, and unreddened. There has not been much time for substellar cluster members to evaporate out of the cluster.

Sherry et al. (2004) showed that the mass function between 0.2 and 1.0 $M_\odot$ is consistent with Kroupa's (2002) field star mass function. They suggested that the mass function may be top-heavy: given the observed numbers of low mass stars, one expects to find more than 10 high mass stars only 1.4% of the time. This conclusion is heavily dependent on how one tallies multiple stars (should σ Ori be considered as one star or six?) Caballero (2007a), on the other hand, found that the mass function between 1.1 and 24 $M_\odot$ has a power law slope of $+2.0^{+0.2}_{-0.1}$, consistent with the Salpeter (1955) slope of +2.3.

The mass function is often parameterized as $\frac{dN}{dM} \propto M^{-\alpha}$. Measurements of α in this cluster are summarized in Table 2. Only the three highest mass samples are spatially complete over a large part of the cluster area. Different studies use diverse selection criteria, but they tend to agree within the (large) uncertainties. There seems to be a trend for a rising mass function (α increasing) with decreasing mass.

Table 2. Summary of published mass functions in the σ Ori cluster. Sherry (2004) finds the mass function is consistent with the Kroupa (2002) field star mass function, which is a sequence of power-law fits.

Mass range ($M_\odot$)	α	Reference
24 – 1.1	$2.0^{+0.2}_{-0.1}$	Caballero (2007a)
1.0 – 0.2	—	Sherry et al. 2004
0.5 – 0.045	1.2±0.2	Tej et al. (2002)
0.2 – 0.013	0.8±0.4	Béjar et al. (2001)
0.11 – 0.006	0.6±0.2	Caballero et al. (2007)
substellar	$0.6^{+0.5}_{-0.1}$	González-García et al. (2006)
substellar	0.4±0.2	Caballero et al. (2007)

6.5. Cluster Mass

Sherry et al. (2004) estimated the total mass of the cluster to be 225±30 $M_\odot$. They fit a field star mass function (Kroupa 2002) to their data between 0.2 and 1.0 $M_\odot$, and then extrapolated the mass function up to 3 $M_\odot$ and down to the substellar mass limit. This yielded 144±28 $M_\odot$. To that they added the mass in the stars with spectral types A0 and earlier (Table 1).

Integrating this mass function, the total number of stars and brown dwarfs in the cluster is about 700 (counting binaries as two objects regardless of separation). This assumes that the binary fraction remains constant with mass, and will be an overestimate if the binary fraction decreases with decreasing mass.

Caballero (2007a) summed the masses of the known members between 1.1 and 24 $M_\odot$ to 100^{+20}_{-19} $M_\odot$, with 46% of that mass in σ Ori itself. He estimated a total mass of about 150 $M_\odot$. Much of the difference between his and Sherry's estimate may arise

from Caballero's assuming a 360 pc distance to the cluster; decreasing the luminosity of the stars by $\sim$ 20% lowers the estimated masses commensurately.

Either way, the mass is too small for the cluster to be gravitationally bound, unless the velocity dispersion of the cluster is much less than the expected (and observed - see Figure 10) velocity dispersion of 1–2 km s^{-1}.

6.6. Age of the Low Mass Population

Age estimates for most clusters are based upon the main sequence turn-off. Blaauw (1964) estimated an 8 Myr age for Orion OB1b based upon the high-mass stars. More recently, Brown et al. (1994) estimated an association age of 1.7 Myr based on Walraven photometry. Since σ Ori Aa is an O9V star (Edwards 1976), the cluster must be younger than $\sim$10 Myr old.

One can also use the temperature of the main sequence turn-on to estimate the cluster age. Sherry et al. (2008) found the turn-on to be near spectral type A0. Cooler cluster members are well above the main sequence (cf. Figure 3). Fitting PMS model isochrones near the ZAMS turn-on yields an age of 2–3 Myr. Age estimates based upon the position of low-mass PMS cluster members on the color-magnitude diagram range from about 2 to 5 Myr (Zapatero Osorio et al. 2002a; Oliveira et al. 2002; Sherry et al. 2004).

Spectra of cluster members in the mass range $0.5 \leq \frac{M}{M_\odot} \leq 0.8$ show no evidence for depletion of Li. This constrains the cluster age to be less than 8 Myr with a most probable age of 2–4 Myr (Zapatero Osorio 2002a). Sacco et al. (2007) did find three stars that showed evidence for Li depletion, but in two cases the Li abundances and the isochronal ages are consistent with membership in the older OB1a association. These stars are likely not members of the σ Ori cluster.

The main source of uncertainty on the age of the cluster is the uncertainty in the distance (which depends in large part on the poorly determined metallicity). Use of the smaller 350 pc distance give systematically larger ages. These age estimates also depend upon the accuracy of low-mass PMS star models at fairly young ages. Baraffe et al. (2002) cautioned that there are significant uncertainties in the model calculations, especially at the younger ages.

6.7. Age Spread

The full effect of high mass stars upon low mass star formation is not known. Do high mass stars trigger or terminate low mass star formation? Discovery of a quantifiable spread in the ages of low mass stars, along with a good age sequence, in an OB association will go far towards elucidating the interactions that drive star formation in a dense environment.

The cluster locus has a small but significant width on the V vs. $V - I_C$ color-magnitude diagram. Sherry (2003) compared the observed width of the cluster locus with the widths of several simulated cluster loci constructed with different star formation histories. He assumed a binary fraction similar to that of field G dwarfs, and that the population was made of naked T Tauri stars with variability amplitudes similar to those observed by Herbst (1994). He concluded that there was no need for an age spread to explain the observed width of the color-magnitude diagram, but an age spread of up to 1 Myr could not be excluded.

Burningham et al. (2005) also examined the possible age spread among members of the σ Ori cluster. They used two epoch R and i' observations of cluster members

taken in 1999 and 2003 to estimate the variability of each cluster member. This method of estimating variability allowed them to include the effects of measurement errors in the variability of each star. They then constructed a series of models with a varying fraction of equal mass binaries. They found that the observed spread on the color-magnitude diagram was too large to be fully accounted for by the combined effects of observational errors, variability (over 1–4 years), and binaries. They concluded that the larger spread on the color-magnitude diagram may be accounted for by either longer period accretion driven variability, an age spread of $\sim$2 Myrs (using a distance of 440 pc, or 4 Myrs using a distance of 350 pc), or a combination of long term variability and a smaller age spread.

6.8. Properties of the Stars

Clusters provide snapshots of stars over a range of masses, at one particular age. Interpreted properly, one can use a sample of clusters of known ages to determine empirically how stellar properties evolve with time. To do so, one must assume that differing environmental effects (e.g., cluster density) and initial conditions are not important.

One property of clusters that may change with time is the binary fraction. Maxted et al. (2008) have examined the spectroscopic binary fraction in the σ Ori and λ Ori clusters. They identify 7 PMS spectroscopic binaries (14.1$< I_C <$16.6) in their σ Ori fields. Based on the γ velocities, five of these are kinematic members of group 2 (the σ Ori cluster), one is a member of group 1, and one has uncertain membership. While their sample reaches to I_C=18.9, they find no binaries in the combined sample with $I_C >$16.6. They conclude that the spectroscopic binary fraction for the bright stars ($I_C <$16.6; M$<$0.1 M$_\odot$) is $0.095^{+0.012}_{-0.028}$, while that of the less massive objects is $<$0.075 at 90% confidence. The suggestion that very low mass stars and brown dwarfs have a spectroscopic binary fraction lower than that of more massive stars has implications for star formation in the cluster environment.

Scholz & Eislöffel (2004) examined the variability of a sample of 23 low mass ($0.07 \leq \frac{M}{M_odot} \leq 0.7$) stars and brown dwarf candidates in the cluster. Sixteen of these are low level variables, with amplitudes $<$0.2 mag at I, which is probably due to rotation. The other 7 objects exhibit T Tauri-like stochastic variability. These also tend to have strong emission line spectra. Rotation periods range from 4 hours to 10 days, with the large-amplitude variables tending to rotate more slowly, consistent with a disk-locking scenario. They concluded that $5 - 7$% of objects in this mass range retain disks at the age of this cluster. Caballero et al. (2004) monitored 28 brown dwarf candidate members for variability on timescales of one hour to 2 years. They found half to be variable, with I-band amplitudes of 0.01 to 0.4 mag. They identified rotation periods of 3-40 hours in 3 objects. They found a correlation between large amplitude variability and the presence of strong Hα emission or IR continuum excesses, which they interpreted as signatures of active accretion. Earlier, Bailer-Jones & Mundt (2001) had found similar results from a variability study of a diverse sample of low mass objects which include 7 members of the σ Ori cluster.

The published X-ray luminosity function (Franciosini et al. 2006) shows that the X-ray emission from the more massive (spectral type K) members of the σ Ori cluster is about a factor of 4 lower than that observed in the Orion Nebula Cluster, or in Cha I, and is comparable to that of ρ Oph. At lower masses (spectral type M), the σ Ori luminosities are below all three other young clusters. This discrepancy can be mitigated

if those candidates not detected in X-rays are actually non-members, and if the distance is increased from 352 to 420 pc (see Sherry et al. 2008).

6.9. Disk Fraction and Active Accretion

Protoplanetary disk lifetimes control the time available for planet formation. The 2–5 Myr age of the σ Ori cluster provides a snapshot of a cluster at an age when disks are beginning to disappear, possibly as a result of planet formation.

Sherry et al. (2004) did not find any evidence for significant near-IR excesses in a $J-H$, $H-K$ color-color diagram. Jayawardhana et al. (2003) conducted a $JHKL'$ survey of several star forming regions, including the σ Ori cluster. They detected $K-L'$ excesses around 2 out of the 6 σ Ori cluster members they observed. Oliveira & van Loon (2004) undertook a mid-IR survey of a diverse sample of objects near σ Ori. Oliveira, Jeffries & van Loon (2004) conducted an L' survey of 28 mostly low mass, likely cluster members. They found that about half the stars retain disks. For an $\approx$3 Myr cluster age, this is consistent with a mean 6 Myr disk survival time. That there are a significant number of stars with nIR excesses at L' and not at K reflects the cool photospheric temperatures of these low mass stars. Oliveira et al. (2006) extended this survey with K and L' imaging of 83 cluster members with $0.04 \leq \frac{\mathrm{M}}{\mathrm{M}_\odot} \leq 1.0$. $K-L'$ color excesses indicate that 27 stars have warm circumstellar dust, for a disk frequency of 33$\pm$6%. They found no significant dependence of the disk fraction on stellar mass.

Hernández et al. (2007) used *Spitzer* IRAC and MIPS colors for a more sensitive study of the disk population. They found that 27% of the members have optically thick disks. Another 7% have evolved disks, that is, transition disks with large inner holes or debris disks. The optically-thick disk fraction is largest in the low mass ($<$1 $\mathrm{M}_\odot$) stars; the evolved disks are most prevalent among the higher mass objects. They found no correlation between X-ray luminosity and disk properties, which suggests that accretion is not a dominant driver of T Tauri X-ray emission. There may be a slight tendency for the fraction of members with circumstellar disks to be enhanced towards the center of the cluster. Overall, the disk fraction in the σ Ori cluster is consistent with the general decrease in disk fraction with cluster age.

Caballero et al. (2007) found that 47$\pm$15% of the lower mass ($0.006 < \frac{M}{M_\odot} < 0.11$) objects have near-IR excesses from optically thisk disks detectable between 1 and 8μm. This disk fraction may be slightly larger than that Hernández et al. found for the low mass stars, extending the general trend for observed disk fraction to increase with decreasing mass. Zapatero Osorio et al. (2007) inferred a disk fraction of about 50% in a sample of 12 planetary mass (7$-$14 M_{Jup}) objects from IRAC 3.6$-$8.0 μm flux excesses. Three of these planetary mass objects identified with disks were earlier tabulated, but not found to have disks, by Caballero et al. (2007). Scholz & Jayawardhana (2008) measured a disk fraction of 29^{+16}_{-13}% in a sample of 18 planetary mass objects ($<$20 M_{Jup}), based on IRAC 8.0μm flux excesses.

One can also use the presence of strong Hα emission (above the level attributable to a stellar chromosphere) as a proxy for accretion, and an active accretion disk. About 8% of the spectroscopically-confirmed PMS stars (spectral types G to K) in the Walter et al. (1998) sample have an Hα equivalent width in excess of 10Å, and appear to be actively accreting at this time. A larger fraction (18%) of the X-ray-selected *Chandra* HRC sample shows Hα emission (Sect 5.1.). Using White & Basri's (2003) criterion, Caballero (2005) estimated that 46^{+16}_{-13}% of the K and M stars are active accretors, although this may be biased since stars with Hα in emission were targeted.

Gatti et al. (2008) estimated mass accretion rates for 31 low mass cluster members with circumstellar disks by using an empirical relation between the Paschen γ line luminosity and the accretion luminosity. The mass accretion rates are about a factor of 10 lower than those measured in the ρ Oph region. This is consistent with viscous disk accretion models (Hartmann et al. 1998).

Caballero (2007a) also noted that the bright B5V member HD 37699 is an IRAS source, and may have a circumstellar disk.

6.10. Globules, Proplyds, and Herbig-Haro Objects

Even fossil star forming regions retain some evidence of their dusty predecessors. The σ Ori cluster is still young, and neighbors the embedded and still active star formation region NGC 2024. Ogura & Sugitani (1998) surveyed Ori OB1b for reflection nebulosities, bright-rimmed clouds, and cometary globules. They cataloged 63 clouds (some of which have multiple discrete components). While most of these are far removed from the immediate region of the cluster, the spatial distribution of the cometary globules resembles a shell of about 1° radius centered near, and with tails directed away from, σ Orionis. These clouds may be the last molecular evidence of the giant molecular cloud that spawned the σ Ori cluster, as it is destroyed by irradiation and winds from σ Orionis itself. See the chapter by Alcalá et al. in this book for more details.

Four Herbig-Haro flows (HH 444–447) are known in the vicinity of σ Ori (Reipurth et al. 1998; Andrews et al. 2004). HH 444 and HH 445 (Figure 11) have extended emission structures which point away from σ Ori. Andrews et al. interpreted these as photoevaporating proplyds. The driving sources include V510 Ori, V603 Ori, and Haro 5-39. Each has a large mid-IR excess (Oliveira & van Loon 2004) indicative of a large circumstellar disk. López-Martín et al. (2001) obtained high resolution spectra of HH 444, and generated a model of the object.

Van Loon & Oliveira (2003) reported the discovery of a mid-IR source, σ Ori IRS1, near, but not coincident with, σ Ori at a projected separation about 3 arcsec ($\sim$ 1000 AU) to the north-northeast. IRS1 is positionally coincident with a radio source (Drake 1990). Caballero (2005, 2007b) reported near-IR and X-ray counterparts to this mid-IR source. It appears to be an evaporating proplyd. This clears up the mystery of why σ Ori appeared to have a strong IR excess.

7. Substellar Mass Objects

The σ Ori cluster has been a rich hunting ground for brown dwarfs. At the 2–5 Myr age of the cluster, brown dwarfs are still bright (K $\sim$14 for a 0.07 $M_\odot$ brown dwarf at 450 pc), and have late-M to mid-L spectral types. This makes them detectable in broad band, wide field surveys.

Béjar et al. (1999) reported the detection of 49 candidate brown dwarfs in a RIZ survey of 870 arcmin^2 region around σ Ori. Zapatero Osorio et al. (2000) reported the detection of three L-type objects with inferred masses between 5 and 15 Jovian masses near σ Ori. Later work (Béjar et al. 2001, 2004a) extended this survey to cover about 1 deg^2. These surveys have found 171 photometrically selected candidate substellar cluster members. Low-resolution optical and near-IR spectroscopy (Béjar et al. 1999, Martín et al. 2001, Barrado y Navascués et al. 2001, 2003) shows that these objects have spectral types between M6 and mid-L with strong Hα emission and weak alkaline lines (due to low gravity) which have been interpreted as indicators of youth. Béjar et

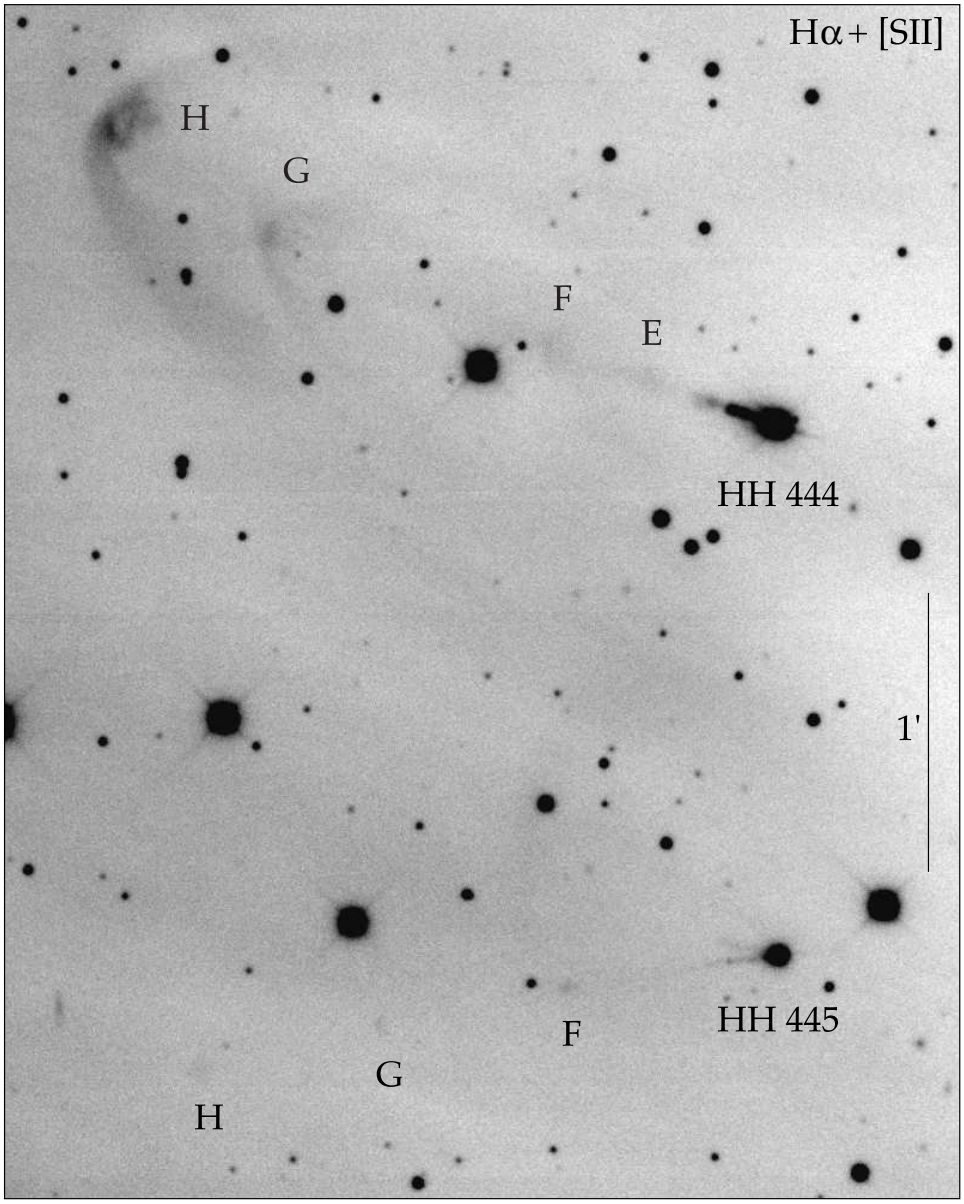

Figure 11. An emission line image (Hα + [S II]) of HH 444 and HH 445. Note the faint bowshocks associated with the easternmost knots. These objects lie east of σ Ori, in the direction of the Horsehead nebula. From Reipurth et al. (1998).

al. (1999) used the models from the Lyon group (Baraffe et al. 1998; Chabrier et al. 2000) to derive masses for the objects in their sample.

González-García et al. (2006) identified 3 planetary mass candidate objects with masses down to 6 Jovian masses near the center of the cluster. Caballero et al. (2007) identified 49 very low mass ($0.006 < \frac{M}{M_\odot} < 0.11$) candidate objects in a deep IJ survey of 790 square arcmin largely southeast of σ Ori AB. Of these, 45 were previ-

ously known. Thirty are considered confirmed cluster members because of near-IR flux excesses or spectroscopic indicators of youth (Hα emission, low gravity, or Li absorption). Statistically, they expect 6 of the remaining 19 to be foreground contamination. At a distance of 360 pc, 33 of these are brown dwarfs and 11 are planetary mass objects. They found no evidence that the mass function turns over at least down to their detection limit, and suggested that the substellar mass objects form via the same physical mechanism that leads to low mass stars.

Zapatero Osorio et al. (2002b) suggested that S Ori 70 (SOri J053810.1 $-$023626) is an $\sim$2–8 M_{Jup} object, and is a free-floating planet. If confirmed, this is the least massive free-floating object yet identified. Martín & Zapatero Osorio (2003) measured the surface gravity, and estimated a 3 M_{Jup} mass and a radius of 0.16 $R_\odot$, independent of the distance to the object. Burgasser et al. (2004) contested this, concluding that it is more likely an old field T dwarf. However, Zapatero Osorio et al. (2008) used a very small proper motion and near-IR colors which are different from field T dwarfs to bolster their argument for membership in the σ Ori cluster, and consequently a low mass. Scholz & Jayawardhana (2008) also find indications of youth and low mass in S Ori 70.

The confirmation of planetary mass objects is of some interest, in that it would provide insights into how very low mass objects (i.e., Jovian mass free-floaters) form. Do they form an extension of the mass function for isolated objects, or do they form as planets, in circumstellar disks, that are then ejected in close encounters in a dense cluster environment? All the masses quoted in this section are derived on the assumption of a distance of 352 pc to the σ Ori cluster. The luminosities and masses are higher for the 420-440 pc distance. While the details of the end of the mass function are uncertain, there are a large number of very low mass objects in this cluster.

8. Summary and Implications

The low mass stars in the fossil star formation regions like Orion OB1b provide a new view into the structure and history of these associations. The numerous low mass stars provide a more complete view of the mass and mass functions, and the spatial extents of the associations, than one can gather from the high mass stars alone. The low mass stars allow one to probe the age spreads and to look for mass segregation within the associations. They provide a more robust measure of the spatial structure of the associations.

The σ Ori cluster, a small part of the Orion OB1b association, contains up to $\sim$225 $M_\odot$ in up to $\sim$700 stars and substellar mass objects. The age is 2–3 Myr; the cluster extends out about 30 arcmin (3.5 pc at a 420 pc distance). The mass function extends from an O9V star to well down into the substellar mass regime. Reddening is low: the mean E($B-V$) is about 0.06 mag. About half the low mass stars have circumstellar disks, and some are still actively accreting. The σ Ori cluster is not gravitationally bound, and will diffuse into the general Orion OB1b association in the astronomically not-too-distant future.

In part because the σ Ori cluster has only recently been recognized, no meta-analysis of all the known members yet exists. Indeed, only recently has a combined list of likely members become available (Caballero 2008c). With a complete membership list, and uniform spectroscopy and photometry, it will be possible to completely char-

acterize the cluster, from its age (and age spread), spatial distribution, and kinematics, to its metallicity and distance, and to the distribution of stellar properties.

The σ Ori cluster is well matched, in terms of total mass, with the cluster surrounding NGC 2024 (Comerón et al. 1996). The NGC 2024 cluster is more highly embedded, appears younger, and has a much higher central density. Comparative studies of the two may help us understand the early evolution of stellar clusters.

The σ Ori cluster is a lower mass and older analog of the Orion Nebula Cluster. In contrast to the Orion Nebula Cluster, which stands out distinctly from its neighbors, the σ Ori cluster today is a part of the large and coeval Orion OB1b association. The apparent simplicity of the ONC may be a matter of perspective – both spatial and temporal. By the time the ONC has aged 2 million years, it will be joined by a myriad of stars and clusters now embedded in the surrounding molecular cloud. Examination of the interplay of the components in these complex regions may tell us whether associations form in pieces - as the agglomeration of clusters forming about the high mass stars - or as a whole.

Acknowledgments. This research has made use of the SIMBAD database, operated at CDS, Strasbourg, France. Star formation research at Stony Brook was supported in part by NSF grant 0307454. We thank the referee, J. Caballero, for many useful comments and suggestions.

References

Abergel, A., Teyssier, D., Bernard, J.P., et al. 2003, A&A, 410, 577
Adams-Wolk, N.R., Wolk, S.J., Walter, F.M., & Sherry, W.H. 2005, in the Poster Proceedings of *Protostars and Planets V*, LPI Contribution No. 1286., 8425
Ambartsumian, V.A. 1947 in *Stellar Evolution and Astrophysics*, Acad. Sci. Armen., Yerevan
Andrews, S.M., Reipurth, B., Bally, J., & Heathcote, S.R. 2004, ApJ, 606, 353
Anthony-Twarog, B.J. 1982, AJ, 87, 1213
Bailer-Jones, C.A.L. & Mundt, R. 2001, A&A 367, 218
Baraffe, I., Chabrier, G., Allard, F., & Hauschildt, P.H. 1998, ApJ, 337, 403
Baraffe, I., Chabrier, G., Allard, F., & Hauschildt, P. 2001, in *The Formation of Binary Stars*, IAU Symp. 200, eds. H. Zinnecker & R.D. Mathieu, ASP, p. 483
Baraffe, I., Chabrier, G., Allard, F., & Hauschildt, P.H. 2002, A&A 382, 563
Barrado y Navascués, D., Zapatero Osorio, M.R., Béjar, V.J.S., et al. 2001, A&A, 377, L9
Barrado y Navascués, D., Béjar, V.J.S., Mundt, R., et al. 2003, A&A, 404, 171
Béjar, V.J.S., Zapatero Osorio, M.R. & Rebolo, R. 1999, ApJ, 521, 671
Béjar, V.J.S., Martín, E.L., Zapatero Osorio, M.R., et al. 2001, ApJ, 556, 830
Béjar, V.J.S., Caballero, J.A., Rebolo, R., et al. 2004a, Ap&SS, 292, 339B
Béjar, V.J.S., Zapatero Osorio, M.R., & Rebolo, R. 2004b, AN, 325, 705
Berghöfer, T.W. & Schmitt, J.H.M.M. 1994, A&A, 290, 435
Blaauw, A. 1964, ARAA, 2, 213
Blaauw, A. 1991, in *The Physics of Star Formation and Early Stellar Evolution*, eds. C.J. Lada and N.D. Kylafis (Dordrecht: Kluwer), p 125
Bohlin, R.C., Jenkins, E.B., Spitzer, L., Jr., et al. 1983, ApJS, 51, 277
Bok, B.J. 1934, Harvard Circ., 384
Bolton, C.T. 1974, ApJ, 192, L7
Briceño, C., Preibisch, T., Sherry, W.H., Mathieu, R.D., Mamajeck, E.A., Walter, F.M. & Zinnecher, H. 2007, in *Protostars and Planets V*, eds B. Reipurth, D. Jewitt, and K. Keil, (Tucson: University of Arizona), p. 345
Brown, A.G.A., de Geus, E.J., & de Zeeuw, P.T. 1994, A&A, 289, 101

Burgasser, A.J., Kirkpatrick J.D., McGovern M.R., McLean I.S., Prato L., Reid I.N., 2004, ApJ, 604, 827
Burningham, B., Naylor, T., Littlefair, S.P., & Jeffries, R.D. 2005, MNRAS, 356, 1583
Caballero, J.A., Béjar, V.J.S., Rebolo, R., & Zapatero Osorio, M.R., 2004, A&A, 424, 857
Caballero, J.A. 2005, AN, 326, 1007
Caballero, J.A. 2007a, A&A, 466, 917
Caballero, J.A. 2007b, AN, 328, 917
Caballero, J.A. 2008a, MNRAS, 383, 375
Caballero, J.A. 2008b, MNRAS, 383, 750
Caballero, J.A. 2008c, A&A, 478, 667
Caballero, J.A., Béjar, V.J.S., Rebolo, R., et al. 2007, A&A, 470, 903
Cameron, L.M. 1985, A&A, 152, 250
Chabrier, G., Baraffe, I., Allard, F., & Hauschildt, P. 2000, ApJ, 542, 464
Comerón, F., Rieke, G.H. & Rieke, M.J. 1996, ApJ, 473, 294
Cunha, K., Smith, V.V., & Lambert, D.L. 1998, ApJ, 493, 195
de Zeeuw, P.T., Hoogerwerf, R., de Bruijne, J.H.J., Brown, A.G.A., & Blaauw, A. 1999, A&A, 117, 354
Drake, S.A. 1990, AJ, 100, 572
Edwards, T.W. 1976, AJ, 81, 245
Flaccomio, E., Micela, G., & Sciortino, S. 2003, A&A, 402, 277
Franciosini, E., Pallavicini, R., & Sanz-Forcada, J. 2006 A&A, 446, 501
Frost, E.B. & Adams, W.S. 1904, ApJ, 19, 151
Fruscione, A., Hawkins, I., Jelinsky, P., & Wiercigroch, A. 1994, ApJS, 94, 127
Garrison, R.F. 1967, PASP, 79, 433
Gatti, T., Natta, A., Randich, S., Testi, L., & Sacco, G. 2008, A&A, 481, 423
González-García, B.M., Zapatero Osorio, M.R., Béjar, V.J.S., et al. 2006, A&A, 460, 799
Greenstein, J.L. & Wallerstein. G. 1958, ApJ, 127, 237
Groote, D. & Schmitt J.H.M.M. 2004, A&A, 418, 235
Haro, G. & Moreno, A. 1953, Bol. Obs. Tonantz. Tacub., 1, 11
Hartkopf, W.I., Mason, B.D. & McAlister, H.A. 1996, AJ, 111, 370
Hartmann, L., Calvet, N., Gullbring, E., & D'Alessio, P. 1998, ApJ, 495, 385
Heintz, W.D. 1997, ApJS, 111, 335
Herbst, W., Herbst, D.K., Grossman, E.J., & Weinstein, D. 1994, AJ, 108, 1906
Hernández, J., Hartmann, L., Megeath, T., et al. 2007, ApJ, 662, 1067
Herschel, W. 1811, Philosophical Transactions of the Royal Society of London, 101, 269
Jayawardhana, R., Ardila, D.R., Stelzer, B, & Haisch, K.E. 2003, AJ, 126, 1515
Jeffries, R.D., Maxted, P.F.L., Oliveira, J.M., & Naylor, T. 2006, MNRAS, 371, L6
Kenyon, M.J., Jeffries, R.D., Naylor, T., Oliveira, J.M., & Maxted, P.F.L. 2005, MNRAS, 356, 89
Kroupa, P. 2002, Science, 295, 82
Landstreet, J.D. & Borra E.F. 1978, ApJ, 224, L5
Lee, T. A. 1968, ApJ 152, 1125
López-Martín, L., Raga, A.C., López, J.A., & Meaburn, J. 2001, A&A, 371, 1118
Lyngå, G. 1981, ADC Bull, 1, 90
Martín, E.L. & Zapatero Osorio, M.R., 2003, ApJ, 593, L113
Maxted, P.F.L., Jeffries, R.D., Oliveira, J.M., Naylor, T. & Jackson, R.J. 2008, MNRAS, 385, 2210
Mokler, F. & Stelzer, B. 2002, A&A, 391, 1025
Morrell, N. & Levato, H. 1991, ApJS, 75, 965
Muzerolle, J., Hillenbrand, L., Calvet, N., Briceño, C., & Hartmann, L. 2003, ApJ, 592, 266
Nakano, M., Wiramihardja, S., & Kogure, T. 1995, PASJ, 47, 889
Ogura, K. & Sugitani, K. 1998, PASA, 15, 91
Oliveira, J.M., Jeffries, R.D., Kenyon, M.J., Thompson, S.A., & Naylor, T. 2002, A&A, 382, L22
Oliveira, J.M., Jeffries, R.D., & van Loon, Th. 2004, MNRAS, 347, 1327

Oliveira, J.M., Jeffries, R.D., van Loon, Th., & Rushton, M.T. 2006, MNRAS, 369, 272
Oliveira, J.M. & van Loon, Th. 2004, A&A, 418, 663
Palla, F. & Stahler, S.W. 1999, ApJ, 392, 667
Perryman, M.A.C., Lindegren, L., Kovalevsky, J. et al. 1997, A&A, 323, 49
Peterson, D.M. et al. 2008, in preparation
Pinsonneault, M.H, Terndrup, D.M., Hanson, R.B., & Stauffer, J.R. 2004, ApJ, 600, 946
Reipurth, B., Bally, J., Fesen, R.A., & Devine, D. 1998, Nature, 396, 343
Reipurth, B. & Bouchet, P. 1984, A&A, 137, L1
Sacco, G.G., Randich, S., Franciosini, E., Pallavicini, R., & Palla, F. 2007, A&A, 462, L23
Salpeter, E.E. 1955, ApJ, 121, 161
Sanz-Forcada, J., Franciosini, E., & Pallavicini, R. 2004, A&A, 421, 715
Scholz, A. & Eislöffel, J. 2004, A&A, 419, 249
Scholz, A. & Jayawardhana, R. 2008, ApJ, 672, L49
Sherry, W.H. 2003, PhD Thesis, SUNY Stony Brook
Sherry, W.H., Walter, F.M., & Wolk, S.J. 2004, AJ, 128, 2316
Sherry, W.H., Walter, F.M., & Wolk, S.J. 2005, in the Poster Proceedings of *Protostars and Planets V*, LPI Contribution No. 1286., 8599
Sherry, W.H., Walter, F.M., Wolk, S.J., & Adams, N.R. 2008, AJ, 135, 1616
Shull, J.M. & van Steenberg, M.E. 1985, ApJ, 294, 599
Tej, A., Sahu, K.C., Chandrasekhar, T. & Ashok, N.M. 2002, ApJ, 578, 523
Turner, D.G. 1976, AJ, 81, 97
Turner, D.G. 1979, PASP, 91, 642
van Loon, J.T. & Oliveira, J.M. 2003, A&A, 405, L33
Walter, F.M., Alcalá, J.M., Neuhäuser, R., Sterzik, M. & Wolk, S.J. 2000, in *Protostars and Planets IV*, eds. V. Mannings, A.P. Boss, and S.S. Russell, University of Arizona, p. 273
Walter, F.M., Wolk, S.J., & Sherry, W.H. 1998, *Cool Stars, Stellar Systems, and the Sun 10*, eds. R. Donahue & J. Bookbinder (ASP: San Francisco), p. 1793
Walter, F.M., Wolk, S.J., Freyberg, M. & Schmitt, J.H M.M. 1997, MmSAI, 68, 1081
Warren, W.H., Jr., & Hesser, J.E. 1977a, ApJS, 34, 115
Warren, W.H., Jr., & Hesser, J.E. 1977b, ApJS, 34, 207
Warren, W.H., Jr., & Hesser, J.E. 1978, ApJS, 36, 497
Weaver, Wm.B. & Babcock, A. 2004, PASP, 116, 1035
White, R.J. & Basri, G.S. 2003, ApJ, 582, 1109
Wilson, R.E. 1953, *General Catalogue of Stellar Radial Velocities* Carnegie Institute, Washington D.C.
Wiramihardja, S., Kogure, T., Yoshida, S., Nakano, M., Ogura, K., & Iwata, T. 1991, PASJ, 43, 27
Wiramihardja, S., Kogure, T., Yoshida, S., Ogura, K., & Nakano, M., 1991, PASJ, 41, 155
Wolk, S.J. 1996, PhD thesis, SUNY Stony Brook
Zapatero Osorio, M.R., Béjar, V.J.S. Martín, E.L., et al. 2000, Science, 290, 103
Zapatero Osorio, M.R., Béjar, V.J.S., Pavlenko, Ya., et al. 2002a, A&A, 384, 937
Zapatero Osorio, M.R., Béjar, V.J.S. Martín, E.L., et al. 2002b, ApJ, 578, 536
Zapatero Osorio, M.R., Caballero, J.A., Béjar, V.J.S., et al. 2007, A&A 472, L9
Zapatero Osorio, M.R., Béjar, V.J.S., Bihain, G., et al. 2008, A&A, 477, 895